

A semianalytical ion current model for radio frequency driven collisionless sheaths

Deepak Bose*, T.R. Govindan, and M. Meyyappan

NASA Ames Research Center, Moffett Field, CA 94035

Abstract

We propose a semianalytical ion dynamics model for a collisionless radio frequency biased sheath. The model uses bulk plasma conditions and electrode boundary condition to predict ion impact energy distribution and electrical properties of the sheath. The proposed model accounts for ion inertia and ion current modulation at bias frequencies that are of the same order of magnitude as the ion plasma frequency. A relaxation equation for ion current oscillations is derived which is coupled with a damped potential equation in order to model ion inertia effects. We find that inclusion of ion current modulation in the sheath model shows marked improvements in the predictions of sheath electrical properties and ion energy distribution function.

* Eloret Corp., Mail Stop 230-3

I. INTRODUCTION

High density, low pressure plasma tools are widely used for etching of semiconductor materials.¹ These tools usually employ a radio frequency (rf) biased electrode on which the wafer is placed. This rf bias controls the impact energies of the ions arriving at the wafer, which can be tuned to attain desirable etch rate and selectivity. The ions are mostly produced by electron impact ionization in the center of the plasma. They are then accelerated toward the substrate and the reactor chamber walls by strong, time-varying electric field in the sub-millimeter scale sheath that is formed at the plasma boundary. Thus, it is important to compute the acceleration of the ions as they traverse the non-collisional sheath in order to predict ion energy distribution (IED) at the wafer. The dynamics of the ions in the sheath is governed by the inertial and electrical forces. The electrons, however, due to their low inertia and high thermalization are in equilibrium with the instantaneous potential and follow a Boltzmann distribution at bias frequencies of interest.

In the absence of a time-varying component of the potential, the ion kinetic energy gain is simply balanced by the drop in the electrostatic potential in the sheath. However, when the rf bias is applied at the electrode, the sheath electric field oscillates in time. This makes a theoretical analysis more complex. Although, a numerical modeling of ion dynamics is possible, it is a formidable task to self-consistently simulate it as a part of a multidimensional reactor model. Hence, it is desirable to have a semianalytical model that allows us to determine the ion impact energies at the wafer and electrical properties of the sheath. This semianalytical model can then be used as a boundary condition in a full reactor simulation.² The expressions for sheath electrical properties are also useful in a plasma-circuit interaction models.³

A theoretical analysis depends on simplifications based on the relative values of the rf bias frequency, ω , and the ion plasma frequency, ω_{pi} (or the ratio $\beta = \omega/\omega_{pi}$), which determines how much the ions respond to the time variation of the sheath potential. If the applied rf bias frequency at the electrode is much different from the ion plasma frequency

the ion dynamics can be considerably simplified. In case of a small applied rf bias frequency compared to the ion plasma frequency ($\beta = \omega/\omega_{pi} \ll 1$), the ions have enough time to fully adjust to the changes in the sheath potential. This is the equilibrium condition where the ion density and velocity at a point in the sheath is only a function of the instantaneous value of the local potential. At the other extreme, when the applied rf bias frequency is much higher ($\beta = \omega/\omega_{pi} \gg 1$), the ions remain in a *frozen* condition as they are unable to adjust to the rapid changes of potential. Under this condition the ion velocity and density can be determined by the local, time averaged value of the potential. Analytical models for the equilibrium and *frozen* conditions have been obtained by various researchers.⁴⁻⁶

In this paper we will focus on the intermediate frequency range when the rf bias frequency is of the same order of magnitude as the ion plasma frequency ($\beta \sim 1$). In this nonequilibrium regime, the ions only partially respond to the time variation of the sheath electric field. This makes an analytical simplification of the ion fluid equations difficult. Riley^{7,8} proposed a unified sheath model for rf driven sheaths that is applicable for all frequencies. In the intermediate frequencies, the ion inertia effects are modeled using a damped potential, \bar{V} , which is obtained from a relaxation equation,

$$\frac{d\bar{V}}{dt} = \frac{V - \bar{V}}{\tau_i}, \quad (1)$$

where τ_i is the ion transit time through the sheath. It was assumed that the ions follow the damped potential instead of the rapidly changing sheath potential, V . This equation is derived by spatially integrating the ion momentum equation.⁷ In order to simplify the analysis and obtain a close form analytical expression for the electric field, the unified sheath model assumes a constant ion current through the sheath at all time. This assumption appears to be rather poor and simplifies the analysis at the cost of accuracy of the model. In Ref. 9, we showed that ion current through a sheath can vary by as much as 70% and has significant effects on the predictions of the electric field, sheath capacitance, IEDs, etc. We then derived a correction term in the expression for the electric field which accounted for the spatio-temporal variation of ion current in the sheath. However, we used

an empirical approach in the above work to determine the magnitude of the ion current oscillations. This restricted the validity of the model to only cases when the sheath potential varies sinusoidally. In this work, we improve this model and propose a modified set of equations that does not depend on empirical expressions and is valid over a wide range of potential and current conditions. We propose a relaxation equation for ion current oscillations which must be integrated in time along with Eq (1).

The rest of this article is organized as follows. In Sec. II, we present the continuum equations that govern ion transport in a non-collisional sheath and the relevant boundary conditions. In Sec. III, we describe the details of the theoretical analysis and the model formulation. In Sec IV, we discuss the results obtained and compare them with the unified sheath model results. Both models are evaluated against the direct numerical solution of the ion transport equations.

II. GOVERNING EQUATIONS

Ions in a non-collisional sheath can be assumed to be non-thermal with high directed kinetic energy. This allows us to use the cold ion fluid equations.

$$\begin{aligned}\frac{\partial n}{\partial t} + \frac{\partial nu}{\partial x} &= 0 \\ \frac{\partial u}{\partial t} + u \frac{\partial u}{\partial x} &= -\frac{e}{m} \frac{\partial V}{\partial x} \\ \frac{\partial^2 V}{\partial x^2} &= -\frac{e}{\epsilon_0} (n - n_e)\end{aligned}\tag{2}$$

n and n_e are the ion and electron number densities, u is the ion velocity, and V is the potential in the sheath. e and m are the unit charge and ion mass respectively. The electrons are assumed to follow a Boltzmann distribution,

$$n_e = n_0 \exp\left(\frac{V}{T_e}\right),\tag{3}$$

where T_e is the electron temperature written in volts and n_0 is the electron (and ion) density at the sheath-presheath edge, where a steady state condition is assumed. We

further assume that the electric field at this boundary is small compared to the fields in the sheath. This enables us to apply asymptotic boundary conditions as described by Riemann and coworkers.^{10,11} For a numerical solution of Eq. (2), the location of the sheath-presheath boundary is immaterial as long as it is sufficiently far away from the electron front. The boundary condition at the sheath-presheath edge is based on quasineutrality and Bohm criterion. Therefore, at $x = -L$ (sheath-presheath boundary),

$$n = n_e = n_0, \quad u = u_B = \sqrt{\frac{eT_e}{m}}, \quad \text{and} \quad V = 0 \quad (4)$$

where, u_B is the ion sonic velocity. A reference potential is chosen at this boundary. Since the ions attain supersonic velocity in the sheath, an extrapolation condition is used for n and nu at the electrode boundary, $x = 0$. In order to close the system, another condition is needed at the electrode boundary which is determined from circuit considerations.

III. SEMIANALYTICAL MODEL

A. Conservation Laws

A particle or ion current conservation law can be obtained by integrating the ion continuity equation [first equation in Eq. (2)]. It is evident that ion conduction current is not necessarily constant in space and time.

$$enu - en_0u_B = -\frac{\partial}{\partial t} \int_{-L}^0 endx = \bar{J}_i \quad (5)$$

The above expression shows that the ion conduction current is dependent on the rate at which the accumulated ion charge in the sheath changes in time. This is expected to be limited by ion inertia. From Eq. (5), we note that ion current has two components; a constant ion current, en_0u_B , entering the sheath from the plasma and a time varying component, \bar{J}_i . \bar{J}_i is an unknown and will be determined later.

The kinetic energy conservation of ions is obtained by integrating the ion momentum equations and defining a damped potential, \bar{V} .

$$\frac{1}{2}mu^2 = \frac{1}{2}mu_B^2 - e\bar{V} \quad (6)$$

The derivation of the above equation is given in Ref. 7. The assumptions made in order to derive this equation are not affected when a time varying ion current is introduced in the analysis. The ion velocity is now conveniently written as

$$\frac{u}{u_B} = \sqrt{1 - \frac{2\bar{V}}{T_e}} \quad (7)$$

The damped potential is determined by integrating Eq (1).

B. Electric Field

The above conservation laws can be used to write the Poisson's equation in the following form

$$\frac{\partial^2 V}{\partial x^2} = -\frac{e}{\epsilon}n_0 \left[\left(1 + \frac{\tilde{J}_i}{en_0u_B}\right) \left(1 - \frac{2\bar{V}}{T_e}\right)^{-1/2} - \exp\left(\frac{V}{T_e}\right) \right] \quad (8)$$

An expression for the electric field can be obtained by multiplying the Poisson's equation by $\partial V/\partial x$ and integrating over the sheath length. This yields,

$$\frac{E^2}{2} - \frac{E_0^2}{2} = I_1 + I_2 + \frac{n_0eT_e}{\epsilon_0} \left[\exp\left(\frac{V}{T_e}\right) - 1 \right], \quad (9)$$

where E_0 is the electric field at the sheath-presheath edge and I_1 and I_2 are the following integrals:

$$\begin{aligned} I_1 &= -\frac{en_0}{\epsilon} \int_0^V \left(1 - \frac{2\bar{V}'}{T_e}\right)^{-1/2} dV', \\ I_2 &= -\frac{en_0}{\epsilon} \int_0^V \left(\frac{\tilde{J}_i}{en_0u_B}\right) \left(1 - \frac{2\bar{V}'}{T_e}\right)^{-1/2} dV' \end{aligned} \quad (10)$$

where V' is a dummy variable in the above integral. We note that Eq (9) is the same expression that is obtained by Riley⁷ with an additional correction term, I_2 . This term accounts for the ion flux oscillations. As expected, I_2 vanishes when the ion current is assumed constant (*i.e.* $\tilde{J}_i = 0$).

In order to evaluate the integrals, I_1 and I_2 , certain simplifying assumptions regarding the spatial variation of \bar{V} and \bar{J}_i are necessary. For \bar{V} we adopt a linear relation, $\bar{V}(x, t) = \alpha(t)V(x, t)$, as proposed by Riley.⁷ $\alpha(t)$ is a function of time. For \bar{J}_i , we assume the following relation,

$$\bar{J}_i(x, t) = \gamma(t)[V(x, t)]^{r(t)} \quad (11)$$

where γ is a constant of proportionality and r is an exponent to be determined later. These quantities are only functions of time. The above relation is necessary in order to evaluate I_2 , its validity, however, can only be justified by the improved performance of the proposed model. The integrals, I_1 and I_2 can now be written as

$$\begin{aligned} I_1 &= \frac{en_0}{\epsilon} \left(\frac{V}{\bar{V}} \right) \left[\left(1 - \frac{2\bar{V}}{T_e} \right)^{-1/2} - 1 \right] \\ I_2 &= -\frac{en_0}{\epsilon} V \bar{J}_i \frac{{}_2F_1(1/2, 1+r; 2+r; 2\bar{V}/T_e)}{1+r} \end{aligned} \quad (12)$$

where ${}_2F_1$ is a hypergeometric function which can be easily evaluated using a summation term as described in Ref. 9. In order to determine the electric field from Eq. (9), the two unknowns, \bar{J}_i and r , must be evaluated.

C. Ion Current

In this section we derive a relaxation equation to determine the ion current oscillations. We begin with the momentum equation for the ions which also can be written as

$$\frac{\partial nu}{\partial t} + u \frac{\partial nu}{\partial x} + nu \frac{\partial u}{\partial x} = -\frac{e}{m} n \frac{\partial V}{\partial x} \quad (13)$$

On multiplying the above equation by unit charge and using the differential of Eq. (5), we get

$$\frac{\partial \bar{J}_i}{\partial t} + u \frac{\partial \bar{J}_i}{\partial x} + enu \frac{\partial u}{\partial x} = -\frac{e^2}{m} n \frac{\partial V}{\partial x} \quad (14)$$

In order to obtain an ordinary differential equation in time, we express the spatial derivatives of u and \tilde{J}_i in terms of the electric field. This is done using the derivatives of Eqs. (6) and (11).

$$\begin{aligned} u \frac{\partial u}{\partial x} &= -\frac{e}{m} \frac{\partial \bar{V}}{\partial x} = -\frac{e}{m} \frac{\bar{V}}{V} \frac{\partial V}{\partial x} \\ \frac{\partial \tilde{J}_i}{\partial x} &= \gamma r V^{r-1} \frac{\partial V}{\partial x} = r \frac{\tilde{J}_i}{V} \frac{\partial V}{\partial x} \end{aligned} \quad (15)$$

From Eqs. (14) and (15), we get the following relaxation equation for the ion current,

$$\frac{\partial \tilde{J}_i}{\partial t} = -\left[\frac{ur \tilde{J}_i}{V} + \left(1 - \frac{\bar{V}}{V}\right) \frac{e^2}{m} n \right] \frac{\partial V}{\partial x} \quad (16)$$

We now identify that $(u/V) \partial V / \partial x \sim 1/\tau_i$, where τ_i is the ion transit time through the sheath. This allows us to simplify this equation further.

$$\frac{d \tilde{J}_i}{dt} = -\frac{(r + g) \tilde{J}_i + g e n_o u_B}{\tau_i} \quad (17)$$

where,

$$g = \frac{e(V - \bar{V})}{\frac{1}{2} m u^2} = \frac{V - \bar{V}}{T_e - 2\bar{V}} \quad (18)$$

The parameter g is the measure of ion nonequilibrium in the sheath and is the driving force responsible for ion flux oscillations. When the ions instantaneously adjust to a relatively slow potential variation (*i.e.* $\bar{V} \approx V$), g becomes small and ion current oscillations become minimal. If $g = 0$ there is no driving force and the ion current oscillations decay. On the other hand when the sheath potential changes rapidly, the high relaxation time, τ_i , prevents the ion flux to respond to the time scale. Thus, Eq. (17) satisfies the general properties of ion current relaxation process in a non-collisional sheath.

D. Solution Technique

In order to close the system, we also need to determine the value of r . It is emphasized that r changes over time, however, its exact dependence on time is unclear. After some

numerical experimentation, we choose $r = r_0 V_w(t)$. This assumes that r is proportional to the potential, V_w , at the electrode over the rf cycle. The constant, r_0 , will be determined iteratively from the periodicity of \tilde{J}_i , which can be written as

$$\int_0^{2\pi/\omega} \frac{d\tilde{J}_i}{dt} dt = 0 \quad (19)$$

The following steps describe the iterative solution technique once n_0 and T_e are obtained from the bulk plasma conditions.

Step 1. Assume initial values of \tilde{J}_i , \tilde{V} , and r_0 .

Step 2. Integrate Eqs. (1) and (17) using a time marching scheme to determine new values of \tilde{J}_i and \tilde{V} . r_0 stays constant until the end of the rf cycle.

Step 3. Repeat Step 2 until the end of the cycle.

Step 4. Compute the new value of r_0 from Eq. (19). If the value of r_0 is converged, go to the next step. Otherwise go to Step 2.

Step 5. Compute ion velocity and the IED from the values of \tilde{J}_i , \tilde{V} , and r over the rf cycle. It usually takes less than 25 cycles to obtain converged values of r_0 . Figure 1 shows that the convergence rate of r_0 is slower at higher values of β . It is also found that the magnitude of the applied potential or current at the electrode does not affect the convergence rate.

IV. RESULTS AND DISCUSSION

In this section we demonstrate that the proposed sheath model with ion flux correction shows improvements in the prediction of the electric field and ion impact energy distribution (IED) at the electrode. We will make comparisons between the present model and the unified sheath model. It must be noted that the unified sheath model is obtained by simply setting $I_2 = 0$ in Eq. (9). These models will also be validated against the numerical solution of the ion fluid equations, which is considered exact in the current analysis.

We will consider two cases; potential control, where a time varying potential waveform is applied as a boundary condition at the electrode, and current control, where a time varying current is passed through the sheath. The results will be analyzed for different

values of the frequency ratio ($\beta = \omega/\omega_{pi}$) at $T_e = 2.0\text{eV}$ with an ion molecular weight of 69 (CF_3^+).

A. Potential Control

We apply a sinusoidal potential waveform at the electrode end of the sheath,

$$V_w(t) = V_{ac} \sin \omega t + V_{dc} \quad (20)$$

where V_{dc} is the dc self bias which is determined by enforcing a net zero current over one rf cycle. The potential is held at zero at the sheath-presheath boundary. A V_{ac} of 100 V is chosen for all cases run in this section. In Fig. 2 we present the ion current oscillation waveform obtained by the present model and the numerical model. A constant ion current assumed in the unified sheath model is also plotted. The ion conduction current is normalized by the ion current entering the sheath from the plasma. There is reasonable agreement between the present model and the numerical solution. The agreement is better at $\beta = 0.1$ and 0.25 than at higher values of β . The overall trends are well captured and the remaining disagreement is attributed to the assumptions made in Eqs. (1) and (11). A further refinement of Eq. (17), which is the subject of future study, could remove some of the existing discrepancies at higher β .

Figure 3 shows the variation of the electric field over the rf cycle. It is evident that the ion flux correction improves the prediction of the electric field values. The amplitude of the oscillations obtained from the unified sheath model is around 25% smaller than the numerical value at $\beta = 0.1$ and 0.25, while the present model consistently shows improved predictions. At $\beta = 1.0$, all three predictions come closer due to a smaller ion flux oscillation. At even higher values of β the correction term is expected to be minimal and, hence, the use of the unified sheath model will be adequate.

Figure 4 shows the IED at the electrode obtained from the numerical and the semianalytical models. It is important to determine the IEDs accurately since they play an important role in the etching process. These distributions are obtained by sampling the ion kinetic energy

over the rf cycle into discrete energy bins. The size of the energy bin determines the noise that appears in the distribution. The ions acquire a bimodal kinetic energy distribution as they travel through a time varying field before they reach the electrode. The two important properties of this distribution are the relative peak heights and the energy gap between the peaks. The energy gap is determined by the range over which the damped potential, \bar{V} , oscillates, which is predicted fairly accurately by both models. It can be seen in Fig. 4 that both the numerical solution and the present model predict a higher high energy peak, while the unified sheath model predicts peaks of equal heights. The unequal peak heights is caused by the ion flux oscillation which weighs in favor of the high kinetic energy ions. During the rf cycle when the sheath potential is at its maximum, the flux of ions is also high, and hence, more ions hit the electrode with high kinetic energies. The reverse is true when the sheath potential drop is at its minimum. It is also interesting to note that at $\beta = 1.0$, the peak heights are not as different as in the case of $\beta = 0.25$. There are two reasons for this. First the ion flux oscillation amplitude is not as high, and second, the phase difference between the ion flux waveform and the potential waveform causes a weaker constructive interference.

B. Current Control

In this case we pass a sinusoidal current through the sheath with no dc component,

$$J = J_{ac} \sin \omega t \quad (21)$$

The sheath potential is obtained as a part of the solution from the following equation,

$$\begin{aligned} J_{ac} \sin \omega t &= enu + J_e + \epsilon \dot{E} \\ &= enu + J_e + \epsilon \frac{\partial E}{\partial V} \dot{V} \end{aligned} \quad (22)$$

where J_e is the electron conduction current. The values of the potential obtained also strongly influences the IEDs. In Fig. 5 we show the sheath potential obtained for $\beta = 0.25$ with the current amplitudes, $J_{ac} = 35$ and 50 A/m^2 . It is evident that the unified sheath

model predicts an exceptionally large value of sheath potential drop than what is obtained from the direct numerical solution of the ion fluid equations. On adding the effect of ion flux oscillations, this unrealistically large potential drop is minimized and the result agrees well with the one obtained from the full numerical solution. This significant change in the potential drop is due to the change in sheath capacitance. In the present model the sheath is allowed to store time varying ion charge unlike the unified sheath model where it is held constant due to a constant ion conduction current assumption. The electric field waveform also shows similar trends. In Fig. 6 we note that the present model predicts values of the electric field that agree with the numerical results extremely well.

Figure 7 shows the IEDs obtained from the two models and is compared with the direct numerical solution results. First we note that in the current control case, the low energy peak is higher than the high energy peak due to the fact that during the rf cycle the sheath potential drop stays near its minimum for a longer time compared to at its maximum [see Fig. 5]. Thus, cumulatively a lot of ions hit the electrode at low energies. Although the ion flux oscillations favor the high energy peak, it is not enough to compensate for this effect. However, the ion flux oscillations do effect the relative peak heights which is evident from a smaller difference in the peak heights in the present model versus the unified sheath model. The major difference is, however, seen in the width of the distribution. This is clearly an artifact of the large sheath potential drop predicted by the unified sheath model, which results in a wider IED spectrum.

V. CONCLUDING REMARKS

We propose a semianalytical ion dynamics model that accounts for ion current oscillations at intermediate bias frequencies ($\beta \sim 1$). A relaxation equation for ion current is obtained which is integrated over the rf cycle along with the equation for the damped potential to determine ion flux, kinetic energy, and sheath potential or current. A correction term is also proposed for the electric field expression. We see marked improvements in electric field and IED predictions when we include the ion current oscillation effect. The biggest improvement is found in the prediction of the sheath potential drop when a specified rf

current is passed through the sheath. This is due to the change in the sheath capacitance since, in this model, the accumulated ion charge is allowed to vary with time in the sheath. The relative peak height and the width of the IED are also improved significantly.

ACKNOWLEDGMENTS

DB's work was supported under NASA contract NAS2-99092 to Eloret.

REFERENCES

- ¹ M.A. Lieberman and A.J. Lichtenberg, *Principles of Plasma Discharges and Materials Processing* (Wiley, New York, 1994). (1986).
- ² M. J. Grapperhaus and M. J. Kushner, J. Appl. Phys. **81**, 569 (1997).
- ³ S. Rauf and M. J. Kushner, J. Appl. Phys. **83**, 5087 (1998).
- ⁴ M.A. Lieberman, IEEE Trans. Plasma Sci. **16**, 638 (1988).
- ⁵ V.A. Godyak and N. Sternberg, Phys. Rev. A **42**, 2299 (1990).
- ⁶ A. Metze, D.W. Ernie, and H.J. Oskam, J. Appl. Phys. **60**, 3081
- ⁷ M.E. Riley, "Unified Model of the rf Plasma Sheath," Sandia National Laboratories Technical Report No. SAND95-0775 UC-401, May 1995.
- ⁸ P.A. Miller and M.E. Riley, J. Appl. Phys. **82**, 3689 (1997).
- ⁹ D. Bose, T. R. Govindan, and M. Meyyappan, J. Appl. Phys. **87** (10), 7176 (2000).
- ¹⁰ K. U. Riemann, Phys. Fluids B **4**, 2693 (1992).
- ¹¹ J. Gierling and K.U. Riemann, J. Appl. Phys. **83**, 3521 (1998).

FIGURE LEGENDS

FIG. 1. Convergence of r_0 with rf cycle at different values of frequency ratios.

FIG. 2. Comparison of normalized ion current, enu/en_0u_B , oscillations at $V_{ac} = 100V$, $T_e = 2.0eV$, and $\beta =$ a) 0.1, b) 0.25, c) 0.5, and d) 1.0 A potential control boundary condition is used.

FIG. 3. Comparison of electric field oscillations at $V_{ac} = 100V$, $T_e = 2.0eV$, and $\beta =$ a) 0.1, b) 0.25, c) 0.5, and d) 1.0. A potential control boundary condition is used.

FIG. 4. Ion energy distribution functions at $V_{ac} = 100V$, $T_e = 2.0eV$, and $\beta =$ a) 0.25 and b) 1.0. A potential control boundary condition is used.

FIG. 5. Comparison of sheath potential at $\beta = 0.25$, $T_e = 2.0eV$, and $J_{ac} =$ a) 35 and b) 50 A/m². A current control condition is used.

FIG. 6. Comparison of electric field at $\beta = 0.25$, $T_e = 2.0eV$, and $J_{ac} =$ a) 35 and b) 50 A/m². A current control condition is used.

FIG. 7. Ion energy distribution at $\beta = 0.25$, $T_e = 2.0eV$, and $J_{ac} =$ a) 35 and b) 50 A/m². A current control condition is used.

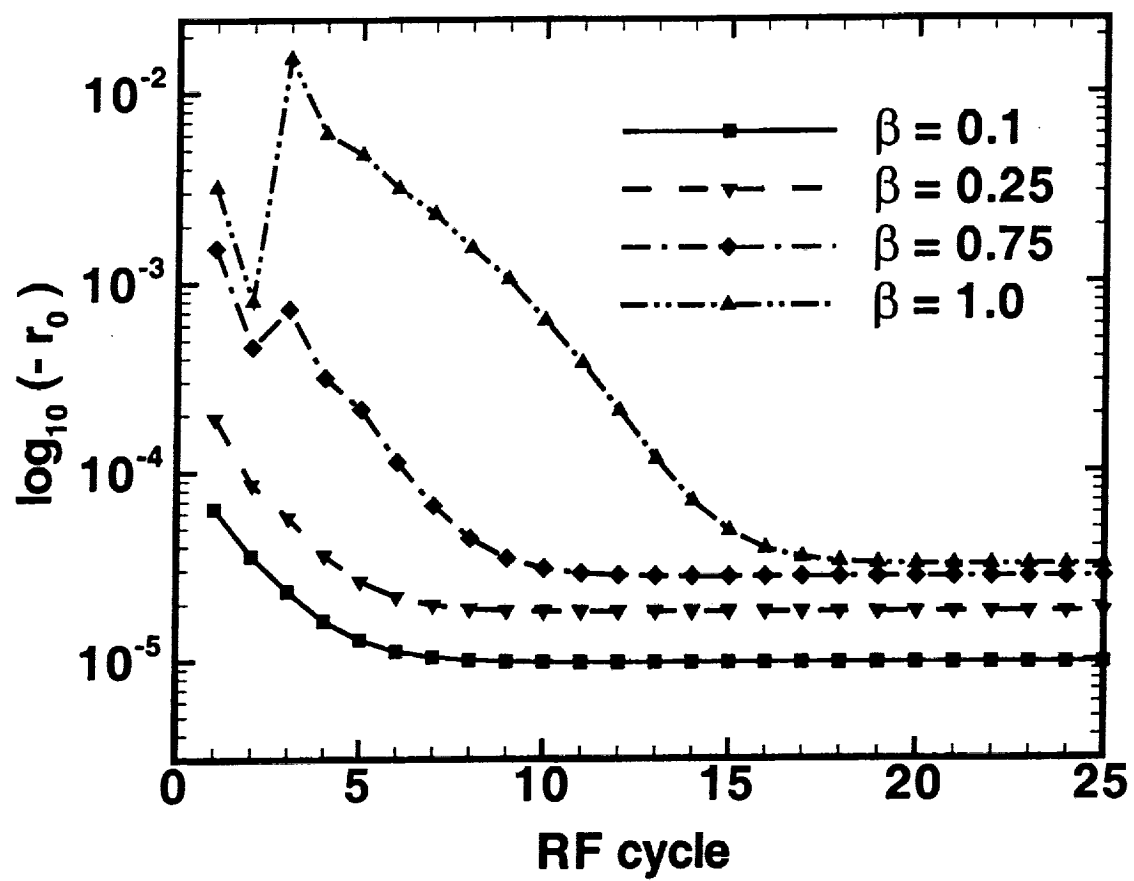


FIG. 1.

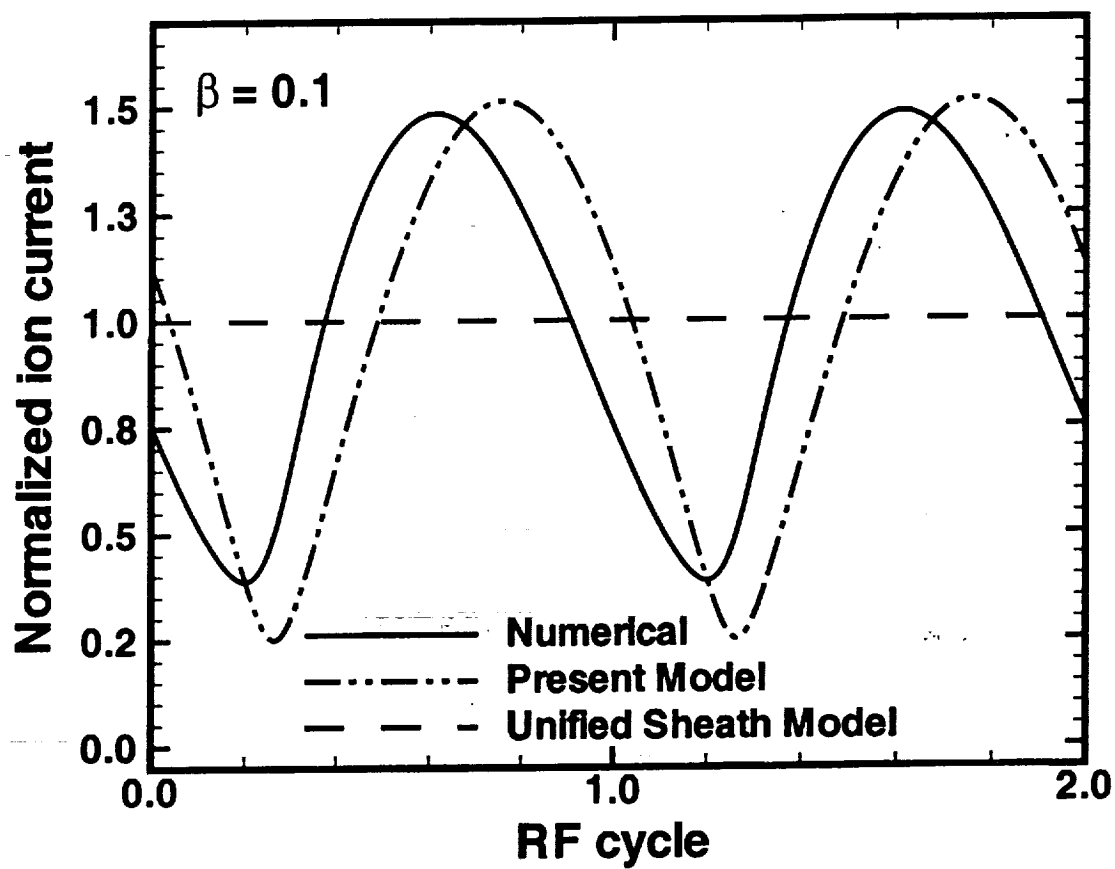


FIG. 2. a)

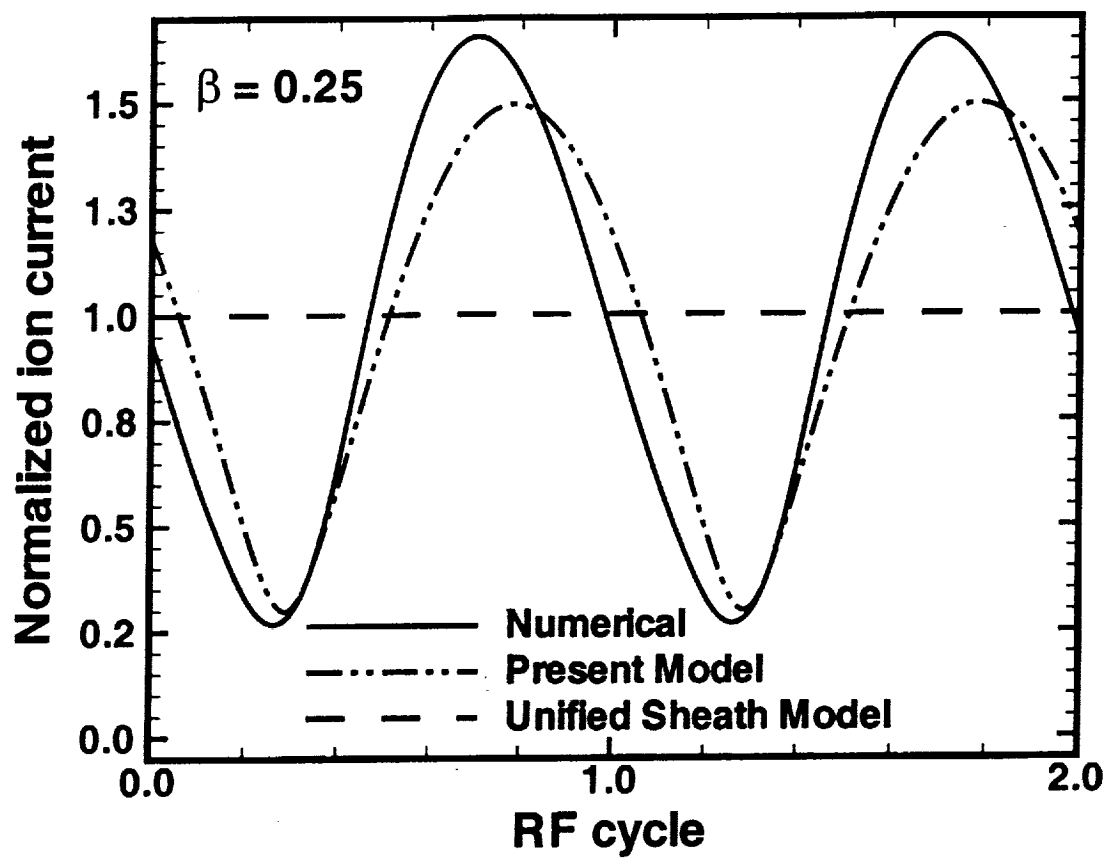


FIG. 2. b)

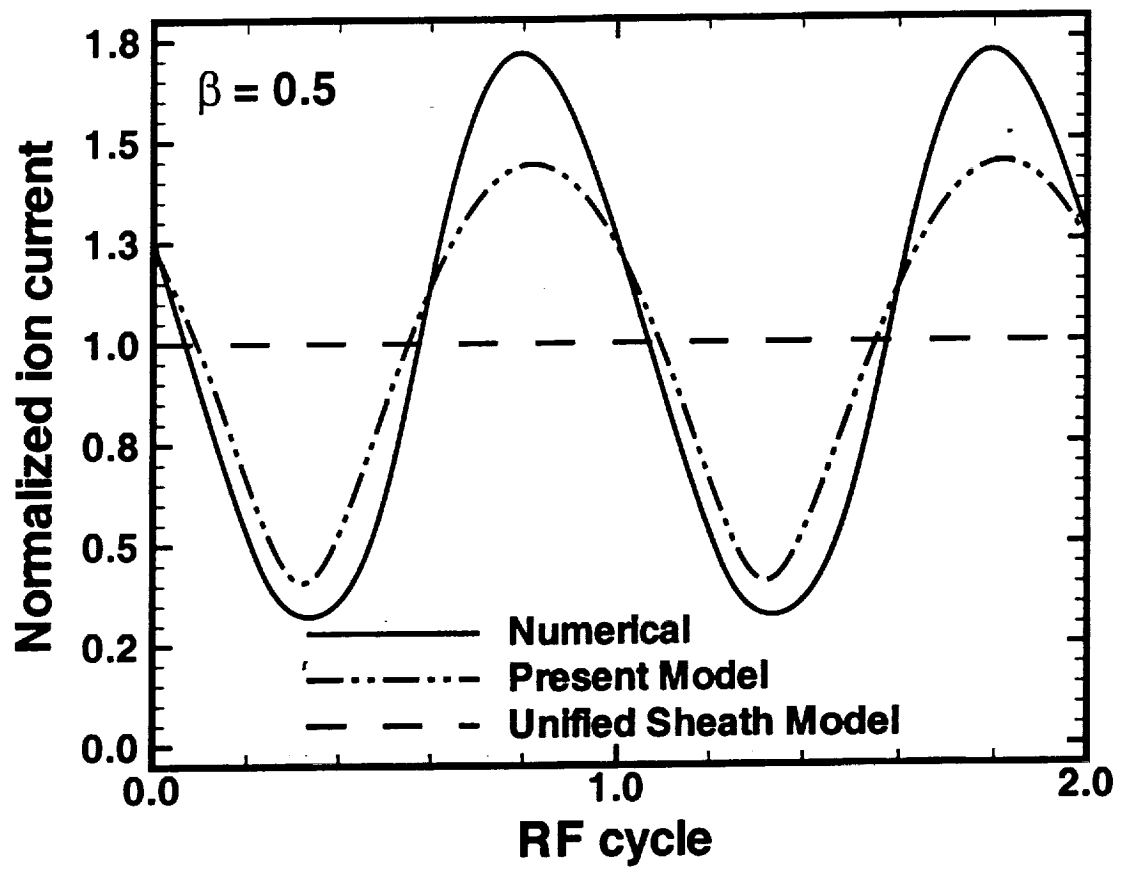


FIG. 2. c)

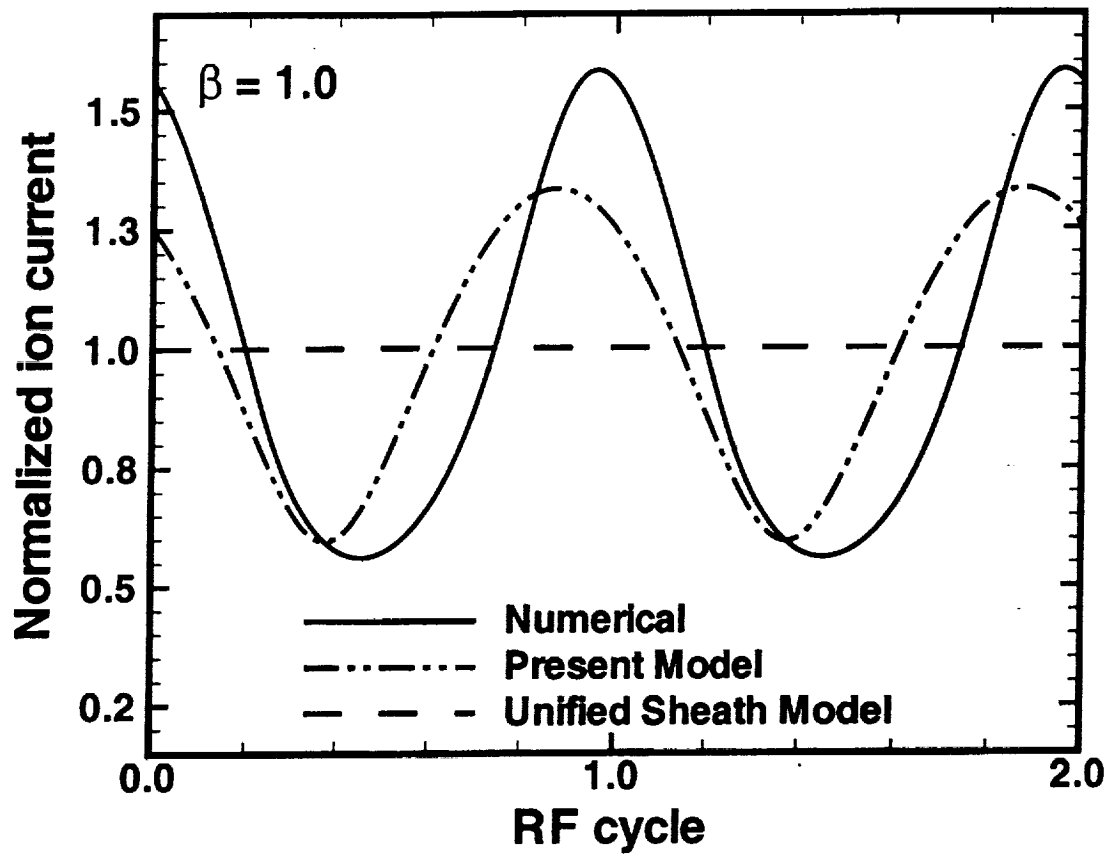


FIG. 2. d)

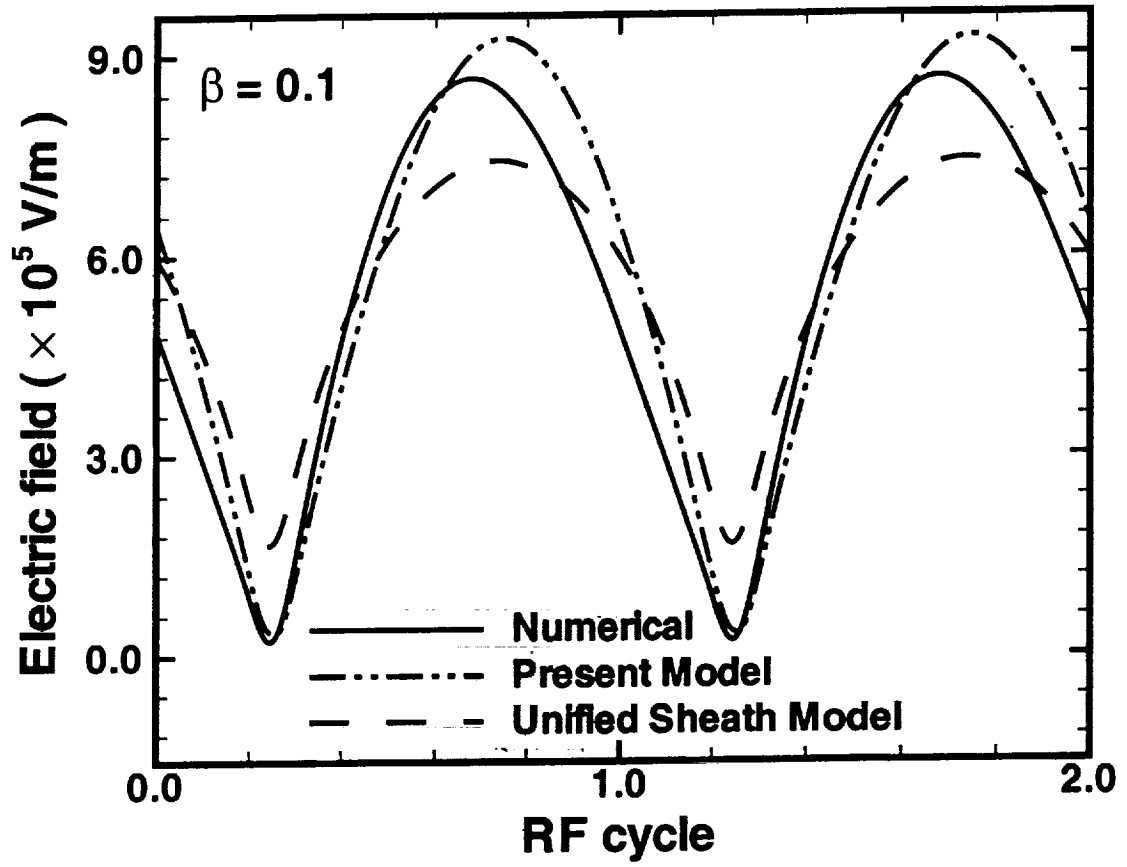


FIG. 3. a)

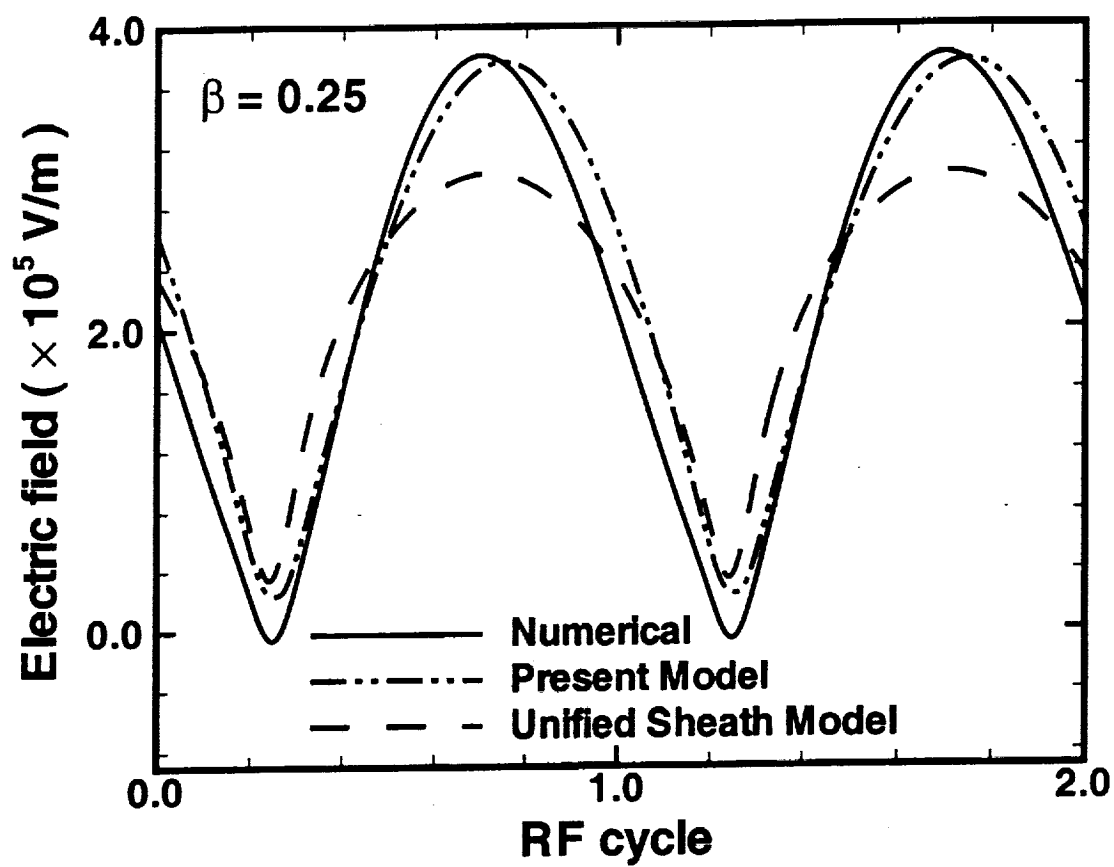


FIG. 3. b)

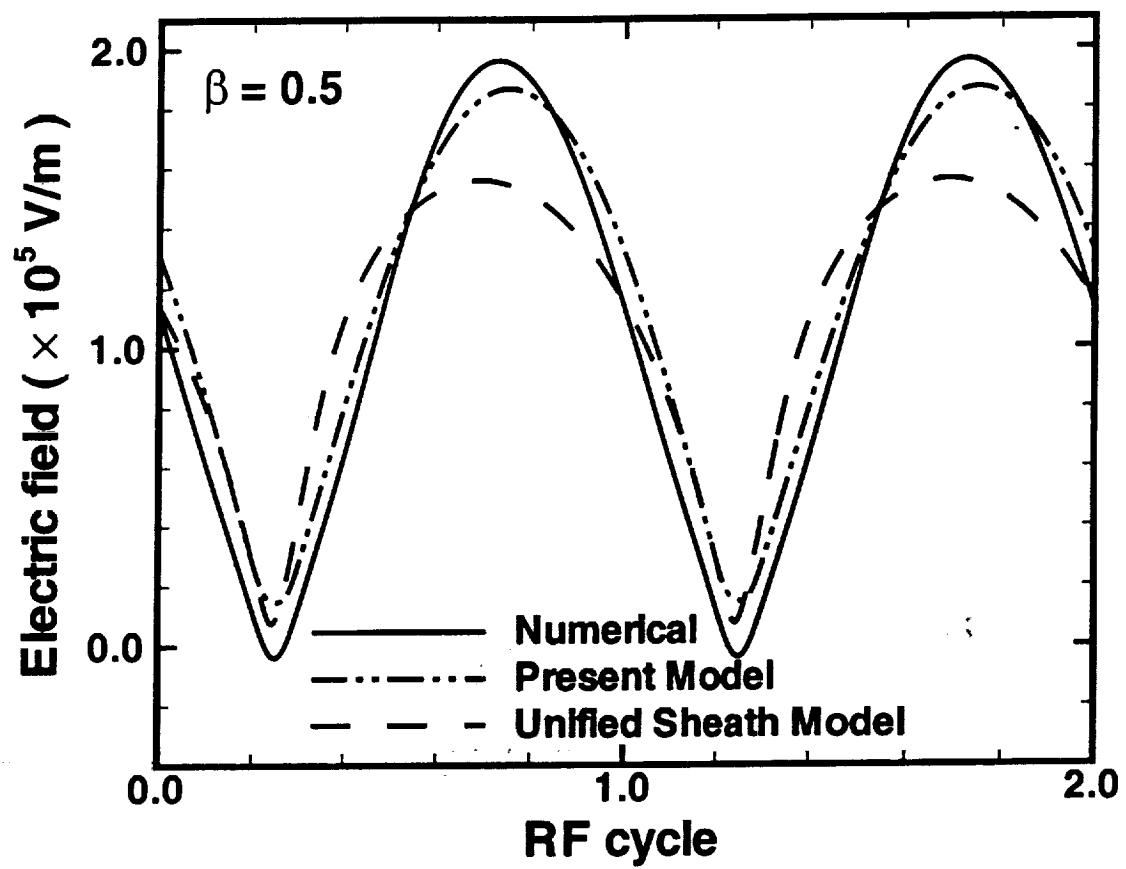


FIG. 3. c)

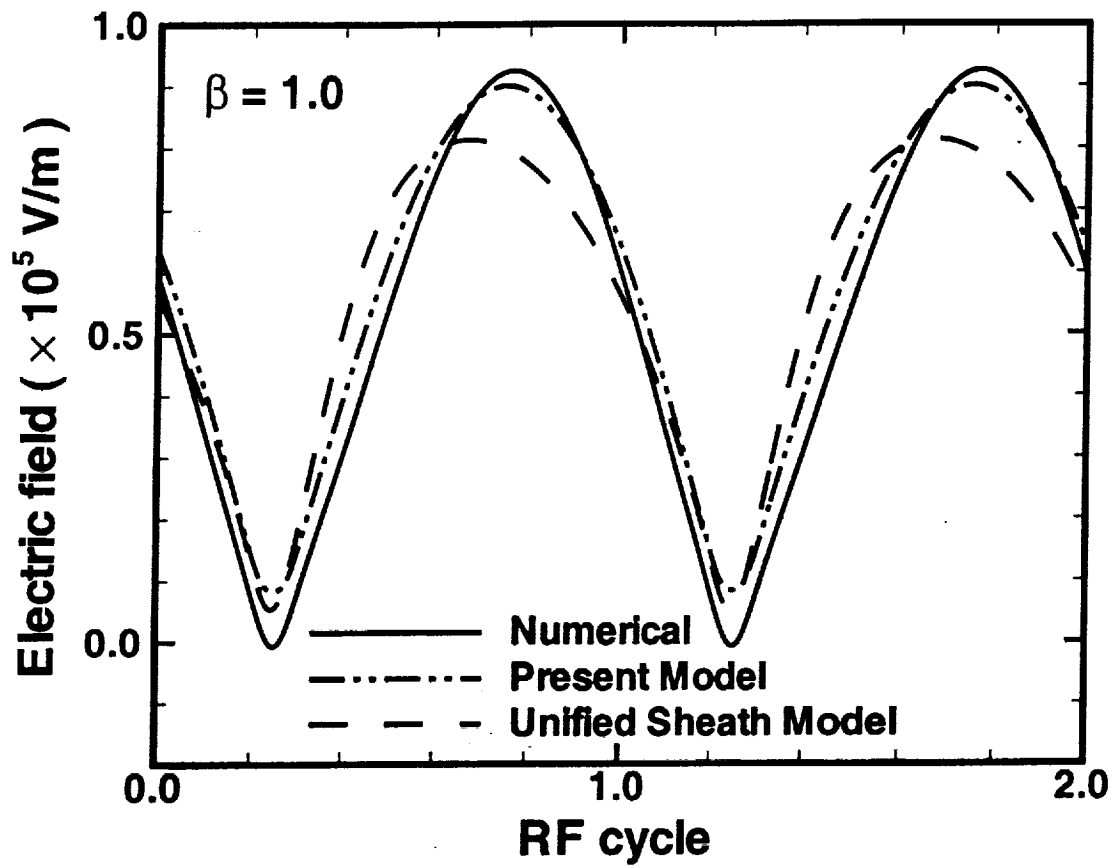


FIG. 3. d)

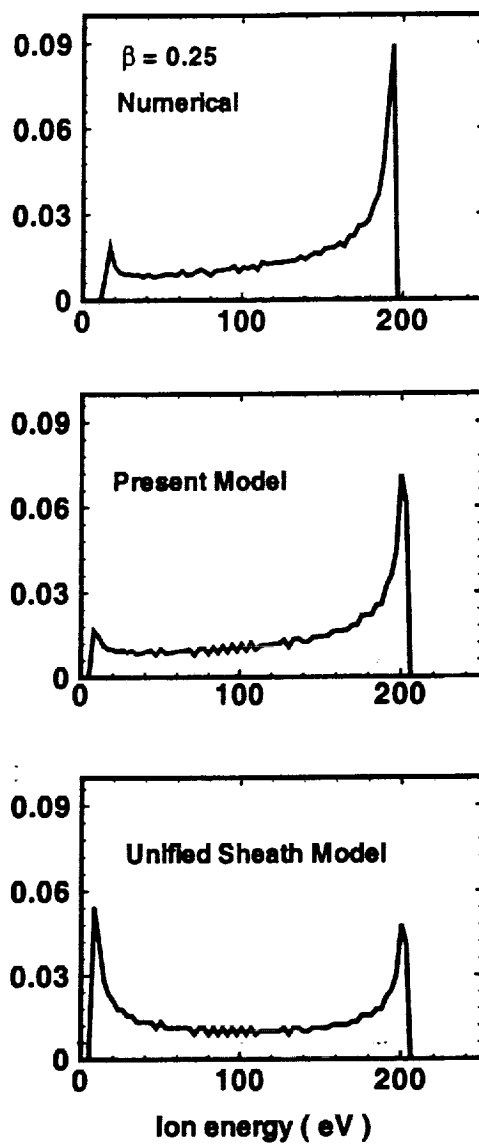


FIG. 4. a)

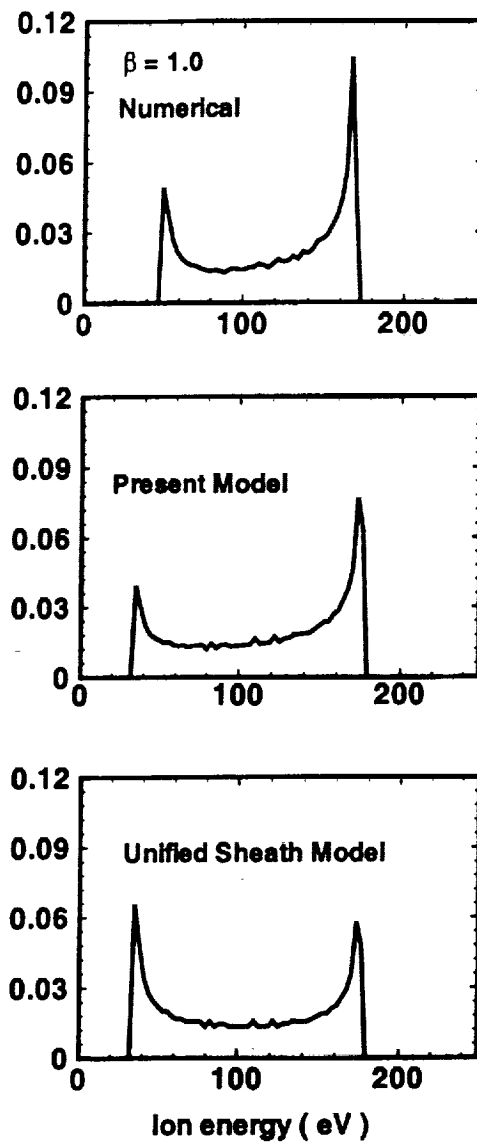


FIG. 4. b)

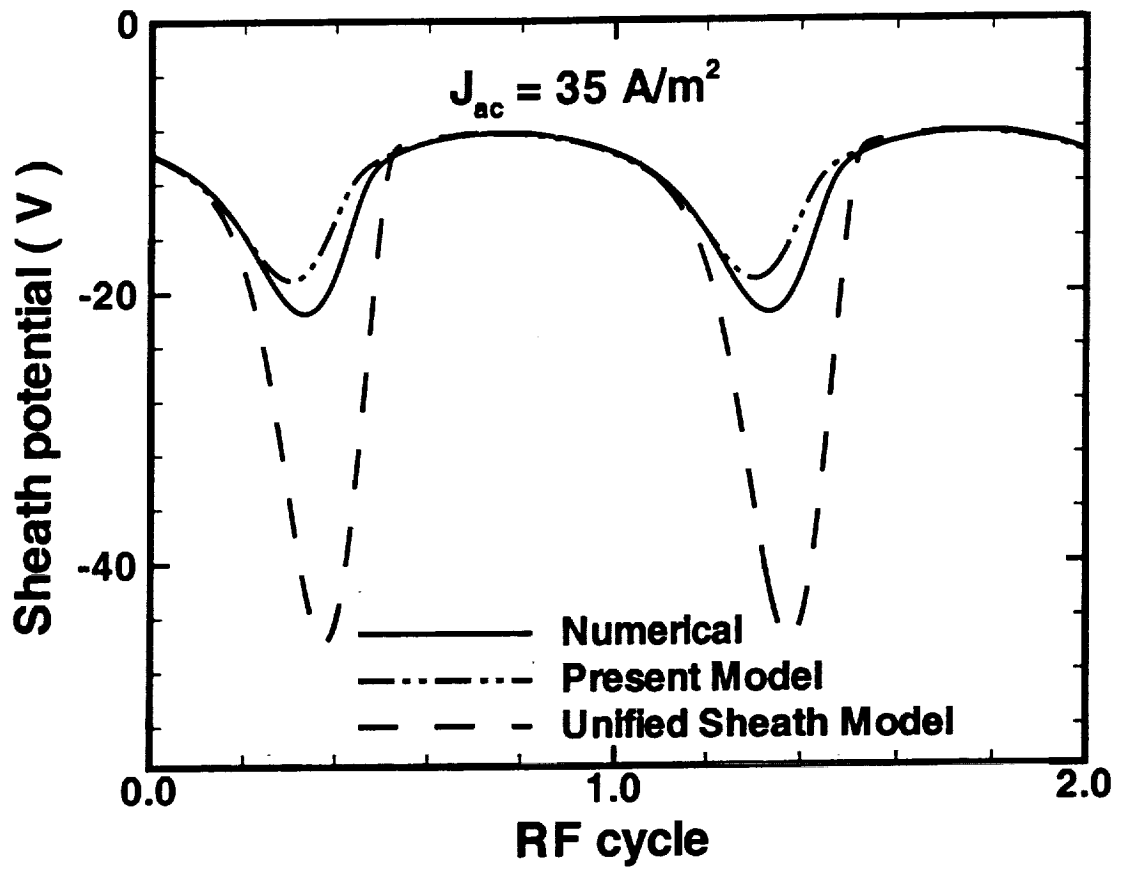


FIG. 5. a)

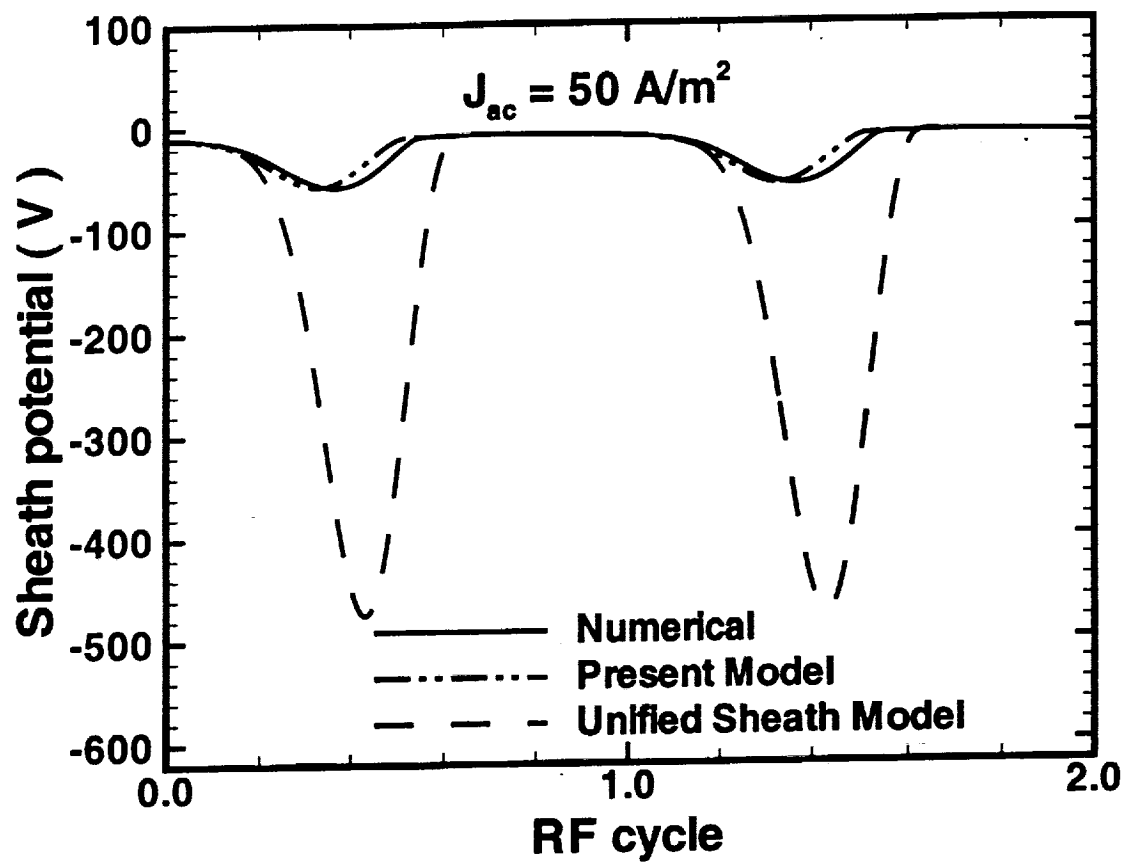


FIG. 5. b)

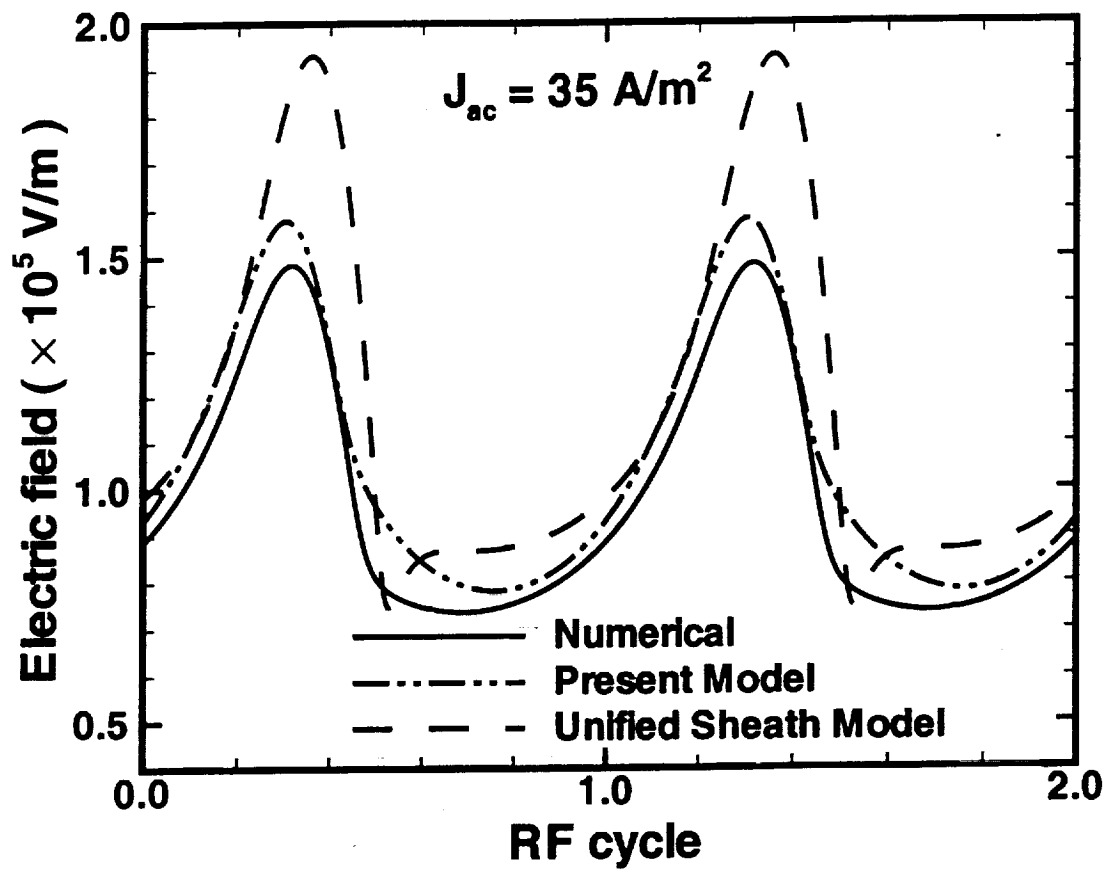


FIG. 6. a)

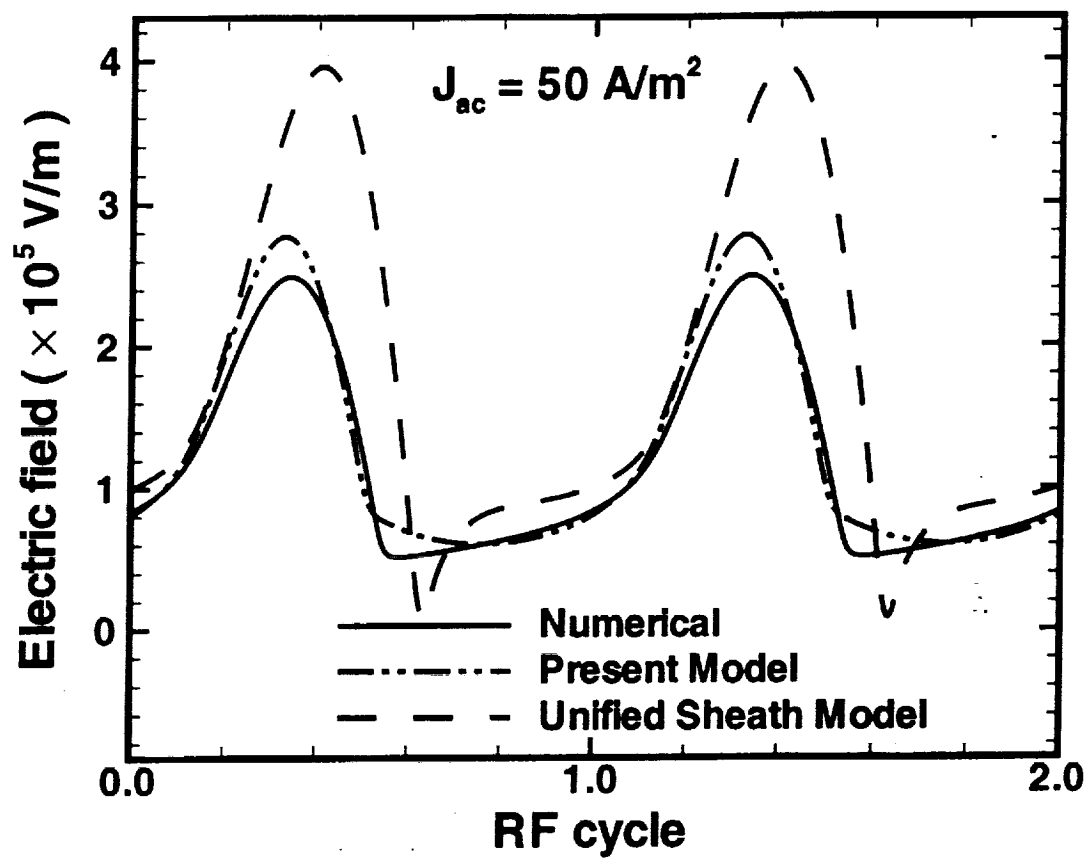


FIG. 6. b)

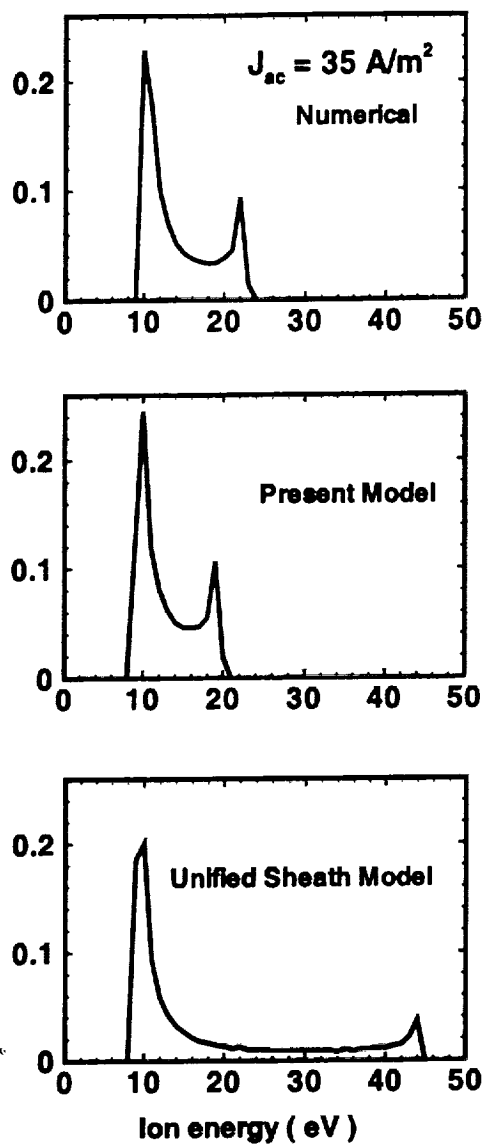


FIG. 7. a)

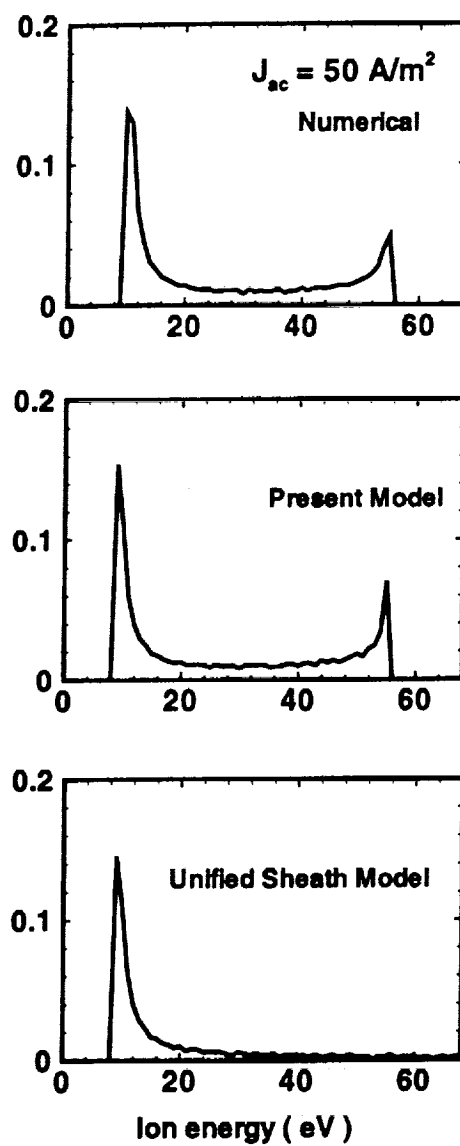


FIG. 7. b)